ADVANCED FUNCTIONAL MATERIALS
www.afm-journal.de

Investigation of Magnetotaxis of Reconfigurable Micro-Origami Swimmers with Competitive and Cooperative Anisotropy

Hen-Wei Huang, Tian-Yun Huang, Michalis Charilaou, Sean Lyttle, Qi Zhang, Salvador Pané, and Bradley J. Nelson**

Recent advances in magnetic nanocomposites have enabled untethered micromachines with controllable shape transformations and programmable magnetic anisotropy, paving the way for a variety of biomedical applications using soft microrobots. Magnetic anisotropy is programmed by assembling the embedded magnetic nanoparticles (MNPs) in polymeric materials to overcome the shape anisotropy of a given structure. However, this approach is questionably effective in reconfigurable structures, as shape changes naturally result in rearrangement of the embedded MNPs. A naturally occurring solution to this problem is found in magnetotactic bacteria, which build chains of MNPs in a linear-chain formation in their cells to create a permanent magnetic dipole moment. This dipole moment enables them to actively sense magnetic fields and coordinate their movement in response, a behavior called magnetotaxis. Inspired by this, self-folding micro-origami swimmers comprising magnetic nanocomposite bilayer structures that exhibit controllable shape transformations and programmable, shape-independent magnetotaxis is fabricated. A study of these structures reveals that their magnetic anisotropy results from competition or cooperation between anisotropy of assembled chains of MNPs and overall shape anisotropy. Moreover, how the magnetotaxis of the reconfigurable micro-origami swimmers depends only on the embedded permanent dipole moment, independent of the overall magnetic anisotropy, is demonstrated.

1. Introduction

The development of magnetically guided microrobots with shape-morphing capabilities facilitates a variety of minimally invasive interventions,[1,2] such as targeted drug deliveries,[3] single cell therapies,[4–6] biopsy using microgrippers,[7] and microtissue transplantations.[8] Understanding the effects of magnetic anisotropy is fundamental for controlling the movement of these untethered micromachines.[9,10] Magnetic anisotropy describes the phenomenon whereby an object's magnetic moment tends to align along the easy axis, which is the energetically favorable direction of spontaneous magnetization. For instance, if a magnetic helical microswimmer is exposed to a magnetic field, the helix will be magnetized along the easy axis (usually the long axis), which will then align with the magnetic field. Under these conditions, in a rotating magnetic field, the helix will not make a corkscrew motion but will tumble.[11] On the contrary, if the helix can be magnetized along its short axis, it will spin around its long axis in corkscrew motion in a rotating magnetic field.[12]

Researchers attempting to program magnetic anisotropy have suggested that magnetically aligning magnetic nanoparticles (MNPs) in polymeric actuators enable the actuator's magnetic anisotropy to be set in any desired direction, thus overcoming the shape anisotropy.[13,14] However, programming magnetic anisotropy in foldable or reconfigurable structures is much more complicated than in static structures, as it requires a thorough understanding of the underlying folding conditions and shape transformations.[15] Once the structure has morphed into another configuration, the relative orientation of MNPs has changed, and the programmed magnetic anisotropy is also altered. Moreover, if the reconfigured shape exhibits higher shape anisotropy, the magnetic anisotropy programmed by the alignment of MNPs can be overcome, which complicates the magnetic control in reconfigurable structures. In nature, magnetotactic bacteria solve this problem by building MNPs in chain configurations to create a permanent dipole moment (PDM) in their cells. This is essentially a tool to sense the Earth's magnetic field, acting as a compass for navigation toward favorable habitats regardless of variation in bacterial morphologies.[16–18]

In this study, reconfigurable micromachines are built from a self-folding hydrogel bilayer structure, allowing us to

Dr. H.-W. Huang, Dr. T.-Y. Huang, S. Lyttle, Dr. S. Pané, Prof. B. J. Nelson
Institute of Robotics and Intelligent Systems
ETH Zurich
CLA H1.1, Tannenstrasse 3, CH-8092 Zurich, Switzerland
E-mail: hhuang@ethz.ch; bnelson@ethz.ch
Dr. M. Charilaou
Laboratory of Metal Physics and Technology
Department of Materials
ETH Zurich
HCI J 496.2, CH-8093 Zurich, Switzerland
Prof. Q. Zhang
School of Electronic Engineering and Automation
Guilin University of Electronic Technology
Guilin, Guangxi 541004, P. R. China
The ORCID identification number(s) for the author(s) of this article can be found under https://doi.org/10.1002/adfm.201802110.

DOI: 10.1002/adfm.201802110

simultaneously program reconfigurable morphologies and magnetic properties by individually forming chains of MNPs in the two layers. The magnetic properties of the reconfigurable micromachines are characterized by studying their hysteresis loops using magnetic fields with small magnitudes. We reveal that the magnetic easy axis is the result of the competition or cooperation between the anisotropy of the assembled chains of MNPs and the anisotropy of the reconfigurable shapes. However, magnetotaxis is determined by the PDM that always runs along the chains of MNPs, due to the local magnetic anisotropy, and it is independent of the global shape of the reconfigurable micromachines. Embedding a PDM in mobile microswimmers enables them to actively sense magnetic fields and coordinate their movement in response, without waiting for their easy axis to be magnetized.

2. Results and Discussion

Hydrogel-based structures with self-folding behavior are achieved by coupling two layers (bimorphs) with different swelling properties. The bimorphs comprise a supporting layer and a thermally responsive layer. MNPs are embedded in both layers for different purposes. The MNPs embedded in the supporting layer are used to program the shape transformations, while the MNPs in the responsive layer determine the overall magnetic properties of the hydrogel bilayers. The reconfigurable morphology of bilayer microstructures is preprogrammed in the supporting layer of flat bilayer structures by magnetically aligning the embedded MNPs. Magnetically aligned MNPs can reinforce the stiffness of the supporting layer in specific directions and induce an anisotropic expansion in hydrogel nanocomposites.[19] We encode the magnetic anisotropy of the self-folded microstructures by aligning the embedded MNPs in the responsive nanocomposites. Two different modes of magnetotaxis are encoded in reconfigurable microswimmers, which are shape-variant and shape-invariant magnetotaxis. Shape-variant magnetotaxis is achieved by horizontally aligning MNPs in the responsive layer in a defined direction. Shape-invariant magnetotaxis is obtained by vertically aligning the MNPs in the responsive layer.

2.1. Programming Reconfigurable Morphologies in Self-Folding Bilayer Structures

Integrating the reinforced supporting layer with a thermally responsive layer with different swelling properties enables the bilayers to fold into desired 3D structures.[20] The initial folding axis is always perpendicular to the alignment of MNPs in the supporting layer because the differential stiffness between the coupled layers is increased by the alignment of MNPs in the supporting layer. The folded shapes are reconfigurable and change in response to external stimuli due to deformations of the responsive layer. In this work, the responsive material poly(*N*-isopropylacrylamide) (PNIPAAm) reacts to thermal stimuli. Therefore, shape transformations are triggered by variations of temperature. As the temperature increases, PNIPAAm dehydrates, and therefore its weight swelling ratio (WSR) decreases.[21] The WSR of PNIPAAm is inversely proportional to the temperature up to the lower critical solution temperature (LCST), which corresponds to 32 °C. Thus, as the temperature increases, the initially folded structures unfold, then fold in the opposite direction around a new axis 90° to the initial folding axis due to the isotropic contraction of the responsive layer.[22]

Figure 1a schematically shows a rectangular bilayer with an alignment of MNPs at a reinforcement angle α_s with respect to the long side. At room temperature, the structure folds into a helix with a helical angle $\theta = 90° - \alpha_S$. When the temperature is higher than the LCST (e.g., body temperature), the WSR of the responsive layer becomes constant, and the refolded shapes reach a steady state with the refolding axis parallel to the alignment of MNPs, and the helical structure refolds into another helix with a complementary helical angle ($\theta = \alpha_S$). Figure 1b shows that rectangular bilayers with aspect ratio L/W = 10 and various α_s fold into 3D structures with corresponding helical angles at room temperature. The 3D structures change their initially folded shapes as the surrounding temperature is increased to 37 °C. The bilayer with $\alpha_s = 90°$ is initially folded into a tube and transforms into a spiral, whereas the rectangular bilayer with $\alpha_s = 0°$ is initially folded into a spiral and transforms into a tube. The rectangular bilayers with $0° < \alpha_S < 90°$ are initially folded into right-handed helices and transform into other helices with a complementary angle but the same chirality. The rectangular bilayers with $-90° < \alpha_S < 0°$ are initially folded into left-handed helices and have the same shape transformation as the right-hand helices. These shape transformations are completely reversible.

2.2. Magnetic Properties Determined by Reinforcing MNPs

Recent work on programming magnetic anisotropy in soft actuators show that the magnetic reinforcing of MNPs in nanocomposites can overcome the shape anisotropy of a structure to effectively overwrite its magnetic easy axis. However, the roles of the magnetically aligned MNPs and the shape anisotropy in the overall magnetic properties of reconfigurable microdevices are still unclear. To understand the effects of magnetically aligned MNPs and shape anisotropy on the magnetotaxis of mobile, reconfigurable microswimmers, we fabricated magnetic nanocomposites with a disc shape and self-folding hydrogel bilayers with a tubular shape.

We systematically study the magnetic properties of thin-film magnetic nanocomposites and self-folded bilayer structures using a vibrating sample magnetometer (VSM) to study their hysteresis loops. A low-magnitude magnetic field ranging from −10 to 10 mT was employed; this is the same as the field applied to align the MNPs during the photopolymerization. Disc-shaped thin-film nanocomposites (DTNs) were chosen because of their in-plane shape anisotropy, which means that they can be magnetized in any direction in the plane of the disc. In **Figure 2**a, we apply the magnetic field in the planar direction of the DTN with uniformly distributed MNPs and measure the induced magnetic moments. The magnetic moments in the disc plane are all oriented along the applied

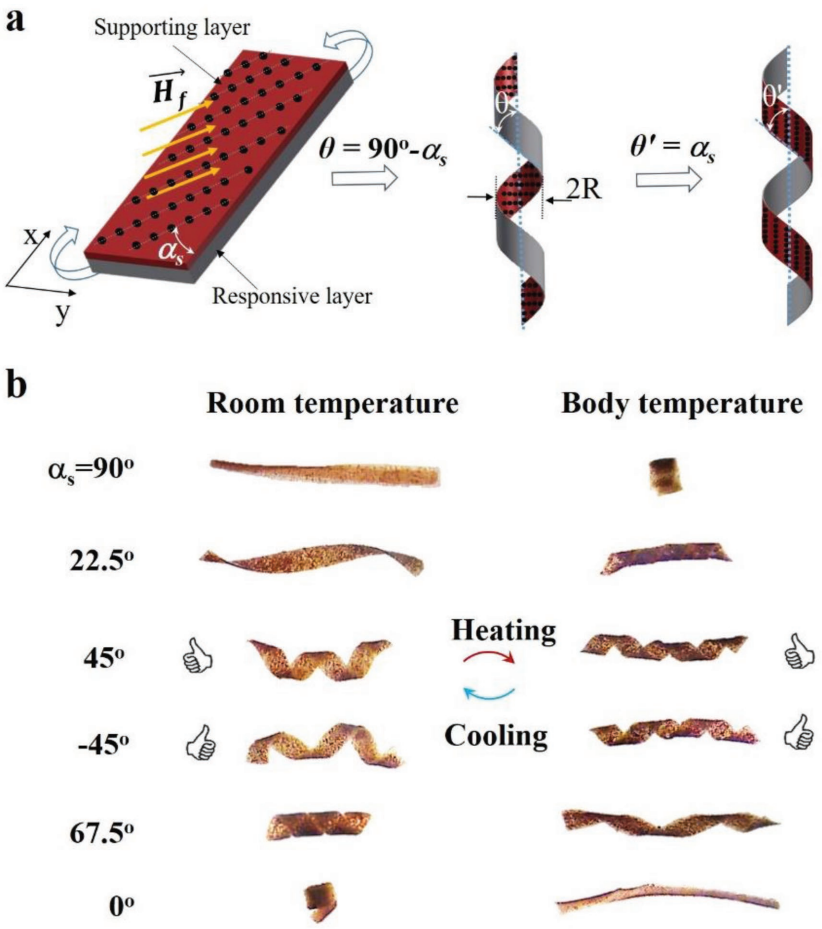

Figure 1. Micro-origami design of the reconfigurable morphologies in self-folding hydrogel bilayers by aligning MNPs in the nonresponsive layer. a) Schematic of aligning MNPs in the nonresponsive layer with an angle α_S gives rise to a 3D helix with helical angle $\theta = 90° - \alpha_S$. The shape transformation triggered by external stimuli (heat) transforms the initially folded shape into a refolded shape with a complimentary helical angle. b) Optical images of the initially folded and refolded hydrogel bilayers.

magnetic field. Switching the magnetic field to the out-of-plane direction, we can compare the hysteresis loop with the in-plane hysteresis loop (Figure 2b; Figure S1, Supporting Information). The difference between the in-plane and out-of-plane cases explains the shape anisotropy of the magnetic properties of the nanocomposite. The in-plane case is more easily magnetized than the out-of-plane direction. Note that the hysteresis loop in this case is defined by the magnetic moment induced by the applied magnetic field.

Next, we study the magnetic properties of DTNs with in-plane magnetically aligned MNPs. We first applied a magnetic field along the alignment axis of the MNPs of the DTN and measured the magnetic moment along this axis, denoted as $M_{\parallel y}$, and orthogonal to the alignment axis, denoted as $M_{\parallel x}$ (**Figure 3**a; Figure S2A, Supporting Information). The results in Figure 3a are similar to those in Figure 2a. We then switched the magnetic field to be orthogonal to the alignment axis and measured the magnetic moments (Figure 3b; Figure S2B, Supporting Information). A strong and permanent magnetic moment ($M_{\perp y}$), generated by the alignment of the MNPs, is observed. If the DTNs are free to move, they will actively align their dipole moment generated by the magnetically aligned MNPs to the external magnetic field. In other words, this permanent magnetic moment is capable of sensing a magnetic field and coordinating movement in response, which demonstrates magnetotaxis.

Figure 4 compares the hysteresis loops for different alignment states of the MNPs, showing that the reinforcing MNPs enlarge the hysteresis loop along the direction of alignment of MNPs, but attenuate the loop orthogonal to the alignment. Therefore, higher magnetization is obtained parallel to the MNPs alignment than perpendicular

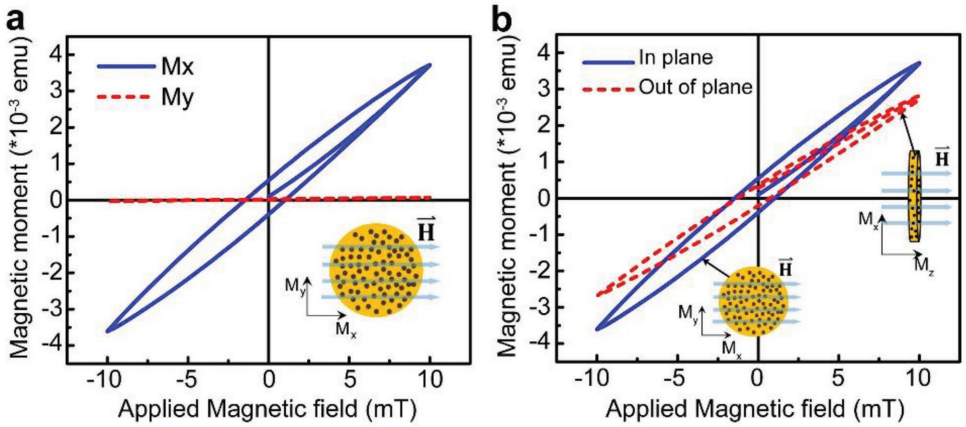

Figure 2. Magnetic characterizations of a disc-shaped nanocomposite with uniformly dispersed MNPs. a) In-plane magnetic moments. b) Comparison of hysteresis loops between the in-plane and out-of-plane directions.

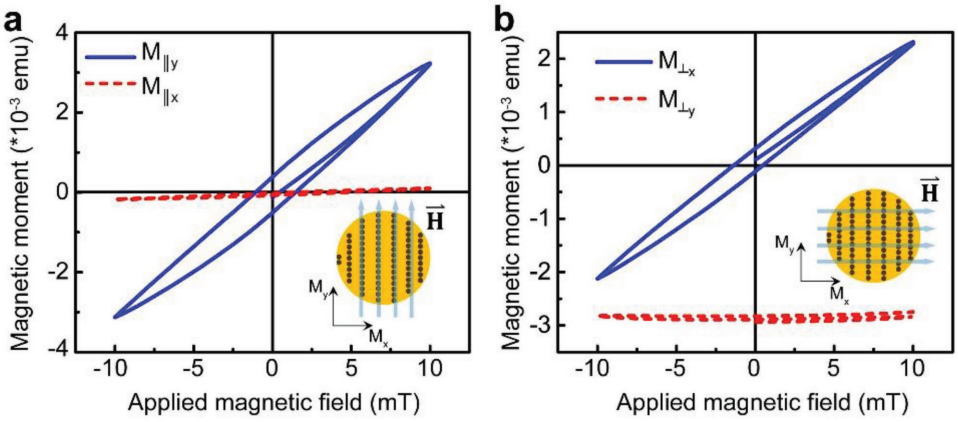

Figure 3. The hysteresis loops of a DTN with in-plane reinforcing MNPs. The measured magnetic moments parallel and perpendicular to the alignment of MNPs when applying a magnetic field a) along the alignment of MNPs and b) orthogonal to the alignment of MNPs.

to it (Figure S2C,D, Supporting Information). The results in Figures 3 and 4 suggest that the magnetically aligned MNPs determine the magnetic easy axis by reinforcing the hysteresis loop and encode the magnetotaxis by generating a PDM.

In an ensemble of MNP, we can model the magnetic state by considering the three major competing forces: 1) the individual magnetic anisotropy of each MNP, 2) the interaction of each MNP with the external field, and 3) the dipole–dipole interactions between MNPs. The outcome of this competition depends on the arrangement of the MNPs: in a scenario where the particles are evenly dispersed (e.g., as shown in **Figures** 2 or **5**a), there is no pronounced net magnetic easy axis and the PDM can be programmed by the external field by saturating the sample. In a scenario where the MNPs are aligned in chains, however, the dipole–dipole interactions along the chain become dominant, provided that interparticle distances in the chain are much smaller than distances between chains,[23] and thus the PDM will always lie in the chain axis. Hence, the PDM will take the form of the chains, as shown in **Figure 6** (see S1, Supporting Information).

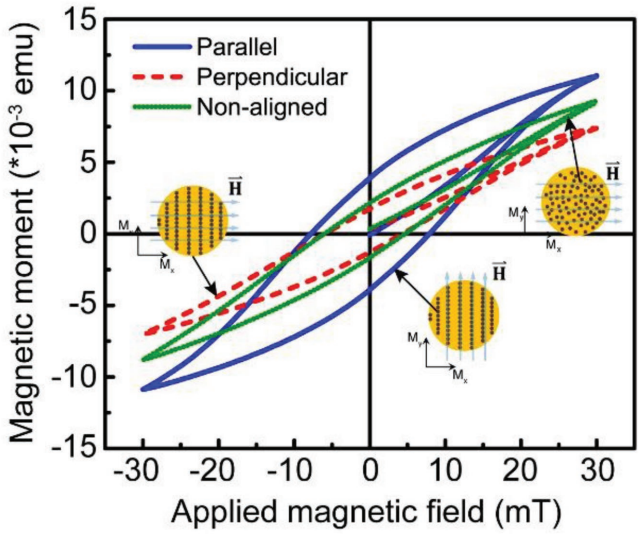

Figure 4. Comparison of hysteresis loops of disc-shaped nanocomposites with and without the alignment of MNPs.

2.3. Encoding Shape-Invariant Magnetotaxis

Based on the understanding of how the magnetic easy axis and PDM are encoded in the DTNs by magnetically aligning MNPs, it is apparent that the alignment of MNPs in the supporting layer used for programming the folding shape also determines the overall magnetic properties of the folded bilayer structures. Morphing the shape will rearrange the reinforcing MNPs, thus changing the easy axis. Moreover, the competition between the reconfigured shape anisotropy and reinforcing MNPs should be taken into account. These coupling effects constrain the magnetic manipulation of shape-morphing microswimmers. As a consequence, microswimmers are forced to change their locomotion when changing their shape.

We now consider whether we can program shape-invariant magnetic properties in the bilayer structures regardless of the alignment of MNPs in the supporting layer by introducing a higher concentration of MNPs into the responsive layer. We hypothesize that the individual alignments of MNPs in the supporting layer and responsive layer could independently program the shape and magnetic anisotropy of the folded structures, respectively. To test our hypothesis, a square bilayer plate with a side length of 3 mm that folds and refolds into a tube with different folding radii was prepared to study the reconfigurable shapes and resulting magnetic properties. The folding shape of the square bilayer plate is determined by the in-plane alignment of MNPs in the supporting layer, and the folding-invariant magnetic property is determined by an out-of-plane alignment of MNPs in the responsive layer (Figure 5a). We believe that the out-of-plane alignment of MNPs in flat bilayer structures will be converted into the radial direction of the folded structures, which is always perpendicular to the folding axis, thus creating a folding-invariant magnetic property.

Figure 5b shows the hysteresis loop of the short axis of the tube when applying a magnetic field along its short axis, and Figure 5c shows the hysteresis loop of the long axis when

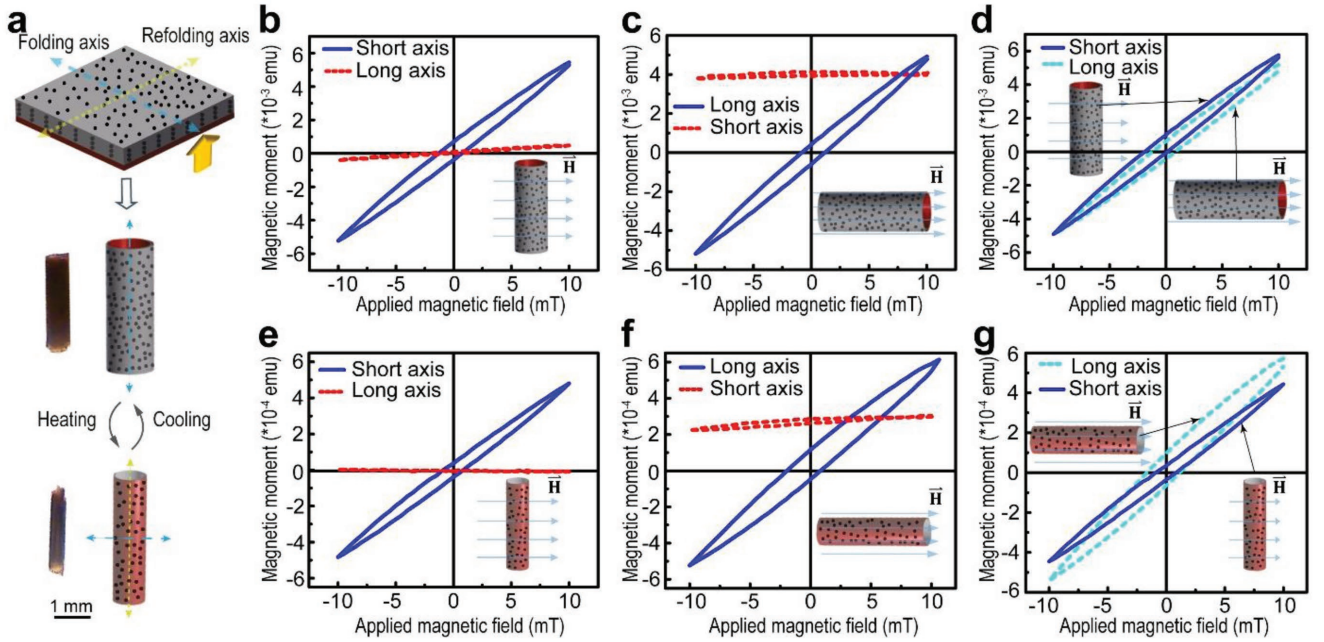

Figure 5. The competition system between the reinforcing MNPs and the shape-invariant magnetotaxis. a) The schematic illustration of a square bilayer plate with out-of-plane alignment of MNPs in the responsive layer folding and refolding into an identical tubular shape. Magnetic characterization of the folded tube encoded with folding invariant magnetic anisotropy in b–d) initial folded state and in e–g) refolded state.

applying the magnetic field in the corresponding direction. We can observe that a strong PDM is created in the short axis. The PDM can be attenuated as the magnetic field perpendicular to the PDM is increased (Figure S3A,B, Supporting Information). Figure 5d compares the hysteresis loops of the long and short axes of the tube. The hysteresis loop of the short axis is similar to that of the long axis because the reinforcing MNPs in the responsive layer is almost compensated by the reconfigurable shape anisotropy along the long axis. These results indicate that the PDM is encoded in the short axis while the magnetic easy axis is blur which can be along either the long axis or the short axis.

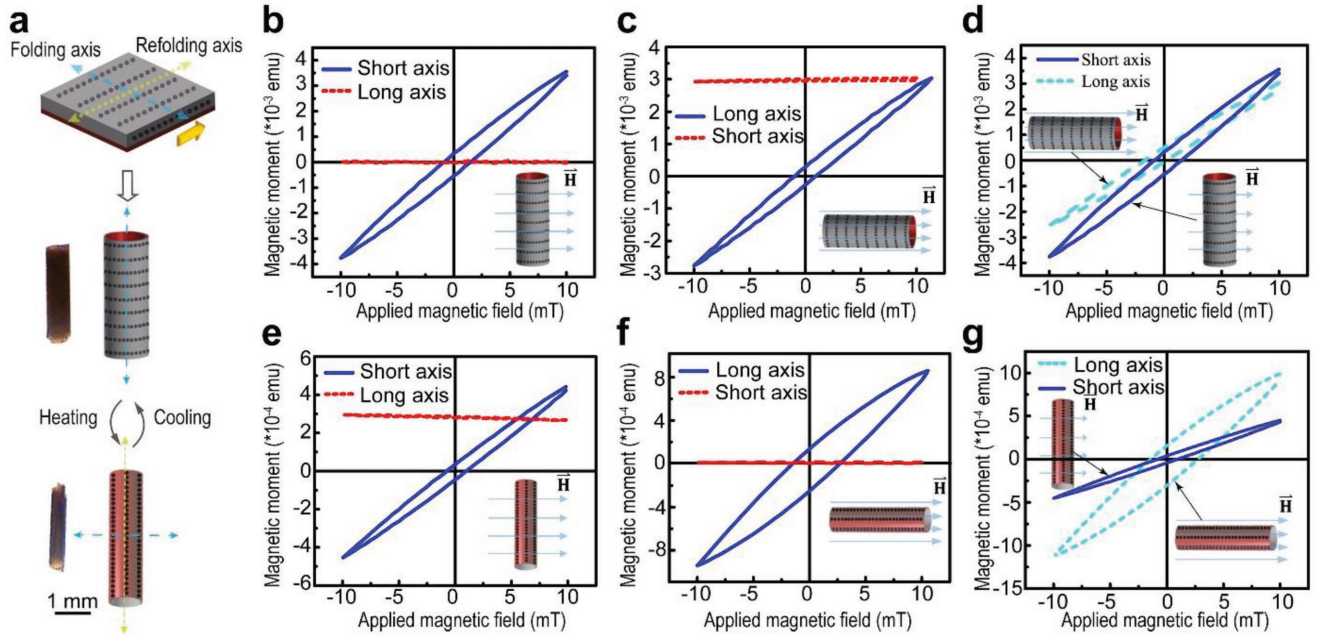

Figure 6. The competition and cooperation system and the shape-variant magnetotaxis. a) The schematic illustration of the reconfigurable tube with the alignment of MNPs in the planar direction of the responsive layer. Magnetic characterization of the folded tube with folding variant magnetic anisotropy. b–d) Measurement of magnetic moments in the initial folded state. e–g) Measurement of magnetic moments in the refolded state.

Next, we refolded a tube that switches its folding axis and exhibits stronger shape anisotropy by increasing the surrounding temperature. The refolded shape was fixed to a sample holder by epoxy glue before the temperature cooled to room temperature. Again, we applied the same magnetic field along the long and short axes of the tube to obtain the hysteresis loops in Figure 5e–g and Figure S3C,D (Supporting Information). The PDM still runs along the short axis. But this time, the hysteresis loop of the long axis becomes greater than that of the short axis because the shape anisotropy is greater than the magnetic anisotropy of the reinforcing MNPs. The PDM does not change when the shape changes because the alignment of MNPs in the responsive layer is still along the radial direction, which results in the folding-invariant magnetotaxis. For a refolded tube with a magnetic easy axis along the long axis and a PDM along the short axis, the long axis is more easily magnetized, but the short axis will actively align with external magnetic fields before the long axis is magnetized if the tube is free to move. This indicates that the PDM determines the magnetic response of mobile, reconfigurable microswimmers, which explains the shape-invariant magnetotaxis of the microswimmers.

2.4. Competition and Cooperation of Anisotropies between Reconfigurable Shapes and Chains of Reinforcing MNPs

We have shown that the magnetic anisotropy set by the alignment of MNPs in a reconfigurable tube can be compensated or overcome by the shape anisotropy. Therefore, it is reasonable to ask whether the MNP alignment can reinforce the shape anisotropy or not. We prepared a bilayer tube identical to the tube encoded with the shape-invariant magnetotaxis, except that the MNPs in the responsive layer were aligned in the same direction as those in the supporting layer. The in-plane alignment of MNPs in the responsive layer is converted into the circumferential direction, which is orthogonal to the initial folding axis. In the refolded tube, the alignment of MNPs is parallel to the folding axis (Figure 6a). Our hypothesis is that both the PDM and magnetic easy axis will be parallel to the short axis in the initially folded tube, and parallel to the long axis of the refolded tube.

As before, we measured the hysteresis loops along the long and short axes of a reconfigurable tube with in-plane reinforcing MNPs in the responsive layer (Figure 6b–d). For the initially folded tube, the PDM lies along the short axis, and the hysteresis loop of the short axis is larger than that of the long axis, which shows the competition between the reinforcing MNPs and the shape anisotropy that endows a magnetization easy direction along the short axis. We then refolded the tube to switch the alignment of MNPs from the circumferential direction to the axial direction. We observed that the PDM in the refolded tube switched from the short axis to the long axis and maintained a similar value (Figure 6e,f). The hysteresis loop of the long axis becomes much larger than that of the short axis (Figure 6g) because the reinforcing MNPs cooperate with the shape anisotropy of the refolded tube along the long axis. Our results suggest that the net magnetic easy axis depends on both MNP orientation and the anisotropy of reconfigurable shapes, whereas the PDM depends only on the orientation of MNPs. Fortunately, the magnetotaxis of microswimmers is determined by the PDM regardless of the shape anisotropy of reconfigurable shapes. The magnetic characterizations of the reconfigurable structures with the shape-variant magnetotaxis by applying higher magnetic fields are shown in Figure S4 (Supporting Information).

2.5. Coordination in PDM and Reconfigurable Morphology Resulting in Multimode Magnetotaxis

Thus far, we have shown that the reconfigurable shapes and magnetotaxis of bilayer structures can be programmed by individually aligning the MNPs in the supporting layer and the responsive layer, respectively. The role of magnetically aligned MNPs in the responsive layer with respect to locomotion is now investigated. Given that, we are able to program reconfigurable microswimmers with different magnetotaxis to achieve any desired locomotion. **Figure 7**a schematically shows that a planar bilayer structure in which the morphology and magnetotaxis have been programmed through the alignment of MNPs in individual layers (described in Cartesian coordinates) can transform into a 3D folded structure (described in cylindrical coordinates). The z-component of the encoded preferential magnetization direction in the planar bilayer will be directly converted to the radial component of magnetic anisotropy in the 3D structure, which is invariant during shape transformations. The x and y components of the encoded preferential magnetization axis anisotropy in the planar structure will be converted into the circumferential components ($\hat{\theta}$ and $\hat{z}$) of the cylindrical coordinates. The encoded magnetic moments of the planar bilayer can be analytically described in Cartesian coordinates as

$$\begin{bmatrix} M_x \\ M_y \\ M_z \end{bmatrix} = M_0 \begin{bmatrix} \cos\vartheta_R \cos\varphi_R \\ \cos\vartheta_R \sin\varphi_R \\ \sin\vartheta_R \end{bmatrix} \quad (1)$$

where M_0 is the magnitude of the overall magnetic moment in the bilayer, φ_R is the angle in the x–y plane with respect to the x-axis, and ϑ_R is the tilting angle with respect to the x–y plane. The self-folding process converts the planar bilayer into a 3D cylindrical structure with predefined α_S. The magnetic moments of the 3D structure can then be described in cylindrical coordinates as

$$\begin{bmatrix} M_{\hat{r}} \\ M_{\hat{\theta}} \\ M_{\hat{z}} \end{bmatrix} = M_0 \begin{bmatrix} \sin\vartheta_R \\ \cos\vartheta_R \cos(\alpha_S - \varphi_R) \\ \cos\vartheta_R \sin(\alpha_S - \varphi_R) \end{bmatrix} \quad (2)$$

The z component of the encoded preferential magnetic anisotropy in the planar bilayer will be directly converted to the radial component $\hat{r}$ in the 3D structure, which is invariant during shape transformations. The x and y components of the encoded preferential magnetization axis in the planar structure will be converted into the circumferential components ($\hat{r}$ and $\hat{z}$) of the cylindrical coordinates.

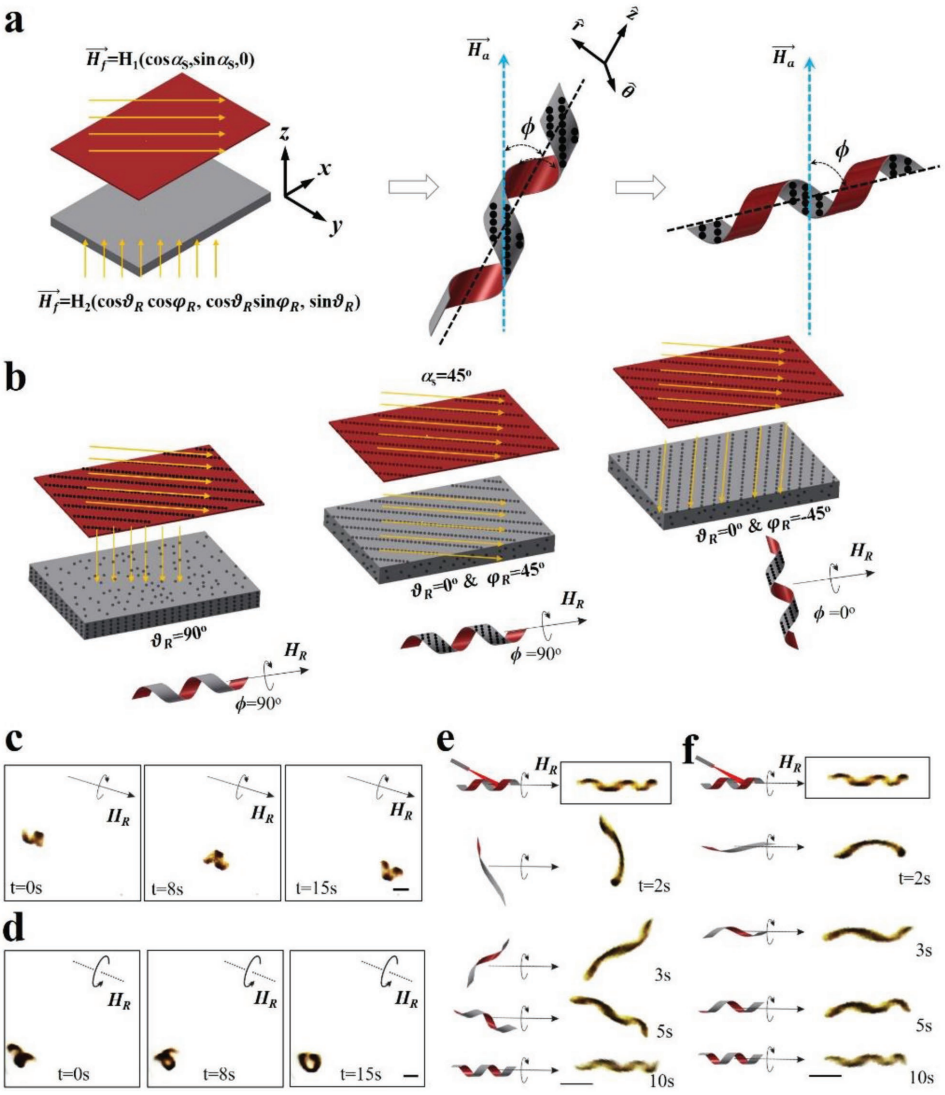

Figure 7. Encoding magnetotaxis in self-folding bilayers through the alignment of MNPs in the thermally responsive layer. a) Independent alignments of MNPs in individual layers for preprogramming folding and magnetotaxis. The encoded magnetotaxis is transformed by shifting the reconfigurable shape. b) The magnetotaxis determines the locomotion of magnetically controlled micromachines. c) Micromachines magnetized in the radial direction perform a wobble-free corkscrew motion rotating at 2 Hz. d) Micromachines magnetized with a misaligned angle (with respect to the short axis) perform tumbling or wobbling motion under a rotating magnetic field (2 Hz). e) Helical microswimmer equipped with folding-variant magnetotaxis changes locomotion under the same external magnetic field. f) Helical microswimmer equipped with folding-invariant magnetotaxis continues corkscrew motion despite the shape transformation. The scale bars all measure 500 µm.

To demonstrate the role that magnetotaxis plays in the locomotion of mobile microswimmers, we fabricated three helical microswimmers with identical self-folded shapes, but encoded them with different magnetization profiles (Figure 7b). A static and uniform magnetic field $\overrightarrow{H_A}$ (20 mT) was applied to verify the magnetic anisotropy of the helical microswimmers. The embedded PDM will automatically align with $\overrightarrow{H_A}$. A misalignment angle ϕ, the angle between the applied magnetic field and the folding axis, can be observed. The misalignment angle can be predicted by $\phi = \cos^{-1}\frac{\hat{z}\cdot\overrightarrow{M_f}}{M_0}$, where $\hat{z}$=[0 0 1] is the folding axis. We use ϕ to briefly describe the programmed magnetotaxis of the micro-origami structures. For instance, a bilayer consisting of a supporting layer with a $\alpha_S = 45°$ folds into 3D helices with helical angle $\theta = 45°$. If these helices are programmed with $\vartheta_R = 90°$ or $\vartheta_R = 0°$ and $\varphi_R = 45°$, the misalignment angle of the helices is $\phi = 90°$. These helical swimmers are able to generate propulsion forces by performing a wobble-free corkscrew motion under a uniform rotating magnetic field (Figure 7c). In contrast, if helices with $\alpha_S = 45°$ are encoded with $\vartheta_R = 0°$ and $\varphi_R = -45°$, the misalignment angle is $\phi = 0°$. In this case, the helical microswimmers perform tumbling or wobbling motion and generate zero net displacement under the same rotating magnetic field (Figure 7d).

We have shown that by appropriately encoding the magnetotaxis in helical microswimmers, optimal corkscrew motion can be achieved. However, these microswimmers are reconfigurable, and the alignment of the MNPs will change according

to the shape transformations. A microswimmer with a shape-variant magnetotaxis is desired for multimode locomotion. For instance, a helix with a PDM along its circumferential direction can be transformed into an identical helix with a PDM along its axial direction. Therefore, the helical swimmer can switch its locomotion back and forth between corkscrew motion and tumbling motion by changing its shape. The magnetization profile of the reconfigured micromachines can be described as

$$\begin{bmatrix} M_{\hat{r}} \\ M_{\hat{\theta}} \\ M_{\hat{z}} \end{bmatrix} = M_0 \begin{bmatrix} \sin \vartheta_R \\ \cos \vartheta_R \sin (\alpha_S - \varphi_R) \\ \cos \vartheta_R \cos (\alpha_S - \varphi_R) \end{bmatrix} \tag{3}$$

For instance, an initially-folded helical microswimmer ($\theta = 45°$ and $\phi = 90°$) with $\vartheta_R = 0°$ and $\varphi_R = 45°$ is heated up by exposure to near-infrared (NIR) light, and the shape refolds to obtain $\theta = 45°$ and $\phi = 0°$. When the NIR is turned off, the microswimmer recovers its initial helical shape. As expected, the locomotion of the helical microswimmers continuously varies with the shape transformation, switching from a tumbling motion to a wobbling motion and finally to a corkscrew motion under a rotating magnetic field. The recovery of shape transformation and locomotion are captured in Figure 7e.

Additionally, in certain situations, one may wish to transform the shape while keeping the same locomotion mechanism. To this end, a shape-invariant magnetic anisotropy is required to maintain the locomotion under the same external control signals. Figure 7f shows that a refolded helix with $\alpha_R = 90°$ recovers its initial shape after the NIR light is turned off. The helix maintains its corkscrew motion in spite of the shape transformation because the PDM always lies in the radial direction of the helical microswimmer (Video M1, Supporting Information). These reconfigurable microswimmers have been tested for more than 50 cycles by exposing to the NIR light without losing the functionalities of the shape changes and magnetotaxis. Figure S9 (Supporting Information) shows that the reconfigurable shapes and the arrangement of the MNPs do not have a visible change after 50 cycles of shape changes.

3. Conclusion

Reconfigurable capabilities enable small-scale machines to perform multiple and versatile tasks. Magnetically guided, self-folded micromachines are able to achieve exceptional locomotion and cargo deliveries by coordinating their reconfigurable morphology with their encoded magnetotaxis. Understanding the effect of reconfigurable shape on magnetic properties is fundamental for controlling the magnetically guided shape morphing micromachines. This work explores the roles of the embedded MNPs and overall shape anisotropy in determining the magnetic properties of reconfigurable microstructures. Our results demonstrate that the magnetic easy axis depends on the competition or cooperation between the anisotropy of the assembled chains of MNPs and the anisotropy of the reconfigured shapes. The magnetically guided locomotion of mobile, reconfigurable microswimmers is dominated by the PDM instead of the magnetic easy axis. Based on the understanding of the magnetic properties of reconfigurable microstructures, we demonstrate that reconfigurable microswimmers encoded with shape-invariant magnetotaxis can maintain the same mode of locomotion regardless of changes in shape. A single robot can thus achieve versatile locomotion modes through coordination between reconfigurable shape and shape-variant magnetotaxis.

4. Experimental Section

Formation of Nanocomposite Pre-Gel Solution: The supporting nanocomposite layer consisted of polyethylene glycol diacrylate (average molecular weight [MW] = 575, polyethylene glycol diacrylate (PEGDA)), photoinitiator 2, 2-dimethoxy-2 phenylacetophenone (99%, 2-dimethoxy-2 phenylacetophenone (DMPA), 3 wt% respect to PEGDA), ethyl lactate (98%, ethyl lactate (EL), 50 wt% respect to PEGDA), and MNPs (Nanostructured and Amorphous USA, 5 wt% respect to the pre-gel solution). The thermally responsive nanocomposite layer was composed of N-isopropyl acrylamide monomer (NIPAAm), cross-linker (PEGDA) (1 wt% respect to NIPAAm), EMPA (3 wt% respect to NIPAAm), EL (70 wt% respect to NIPAAm), and MNPs (10 wt% respect to the pre-gel solution). Pre-gel nanocomposite solutions were subjected to sonication for 20 min to obtain a dispersion of the MNPs.

Formation of the Bilayer Structure: For both layers, the pre-gel solution was filled into a configurable chamber consisting of a glass photomask, and an SU-8 spacer on a silicon substrate. The SU-8 spacer defined the thickness of the layer. The 2D patterns of the hydrogel bilayers were defined by a glass mask. The thicknesses of the supporting layer and the thermally responsive layers were 10 and 30 µm, respectively.

For the supporting layer, a uniform magnetic field with an intensity of 10 mT was applied for 1 min to align the MNPs in a particular direction to regulate the internal stress distribution, thus defining the folding axis of the hydrogel bilayers. Subsequently, the nanocomposite solution was photopolymerized by UV light (20 mW·cm^{-2}) for 30 s while maintaining the applied magnetic field.

For the thermally responsive layer, a uniform magnetic field with the same intensity of 10 mT was applied in a defined horizontal direction or a vertical direction for 1 min to determine the magnetotaxis. Subsequently, the thermally responsive nanocomposite was exposed to UV light for 1 min. The thermally responsive layer was polymerized on top of the supporting layer, thus forming a bilayer structure. Further details on the fabrication processes of the hydrogel bilayers and the setups for programming their magnetic anisotropy can be found in ref. [15].

Characterization of Magnetic Properties of Reconfigurable Microstructures: DTNs were obtained from a nanocomposite thin film with a thickness of 100 µm (before swelling), formed by using a biopsy punch with a diameter of 5 mm. The initially self-folded tubes were obtained from a square bilayer with a side length of 3 mm. Refolding tubes were used to demonstrate reconfigurable morphologies and the corresponding magnetic anisotropy. The refolding of the tubes was attained by heating up the initially folded tubes to 37 °C, causing them to refold in the opposite direction and along the opposite axis. An NIR laser was used to heat up the magnetic nanocomposites. The magnetic characterization was realized at 25 °C by using a VSM. The refolded shape of the tubes obtained at 37 °C was fixed by gluing them to a sample holder during the VSM measurements at 25 °C. The resulting magnetically mobile micromachines were manipulated by applying rotating magnetic fields using a custom-built electromagnetic system, Octomag.[24]

Supporting Information

Supporting Information is available from the Wiley Online Library or from the author.

Acknowledgements

This work was financially supported by the European Research Council Advanced Grant Soft MicroRobots (743217), the Swiss National Science Foundation (no. 200021_165564), the National Natural Science Foundation of China (11702003), and the China Postdoctoral Science Foundation (2016M600861). The authors are thankful to Dr. Naveen Shamsudhin and Dr. Jin Zhang for helping in the experiments of VSM measurement, to Dr. Eva Pellicer and Prof. Jordi Sort for discussion, and to the FIRST lab of ETH Zurich for technical support.

Conflict of Interest

The authors declare no conflict of interest.

Keywords

magnetism, microswimmers, origami, reconfigurable structures, soft matter

Received: March 25, 2018
Revised: May 27, 2018
Published online: July 23, 2018

[1] M. Sitti, H. Ceylan, W. Hu, J. Giltinan, M. Turan, S. Yim, E. Diller, *Proc. IEEE* **2015**, *103*, 205.
[2] B. J. Nelson, I. K. Kaliakatsos, J. J. Abbott, *Annu. Rev. Biomed. Eng.* **2010**, *12*, 55.
[3] J. Li, B. Esteban-Fernández de Ávila, W. Gao, L. Zhang, J. Wang, *Sci. Rob.* **2017**, *2*, 1.
[4] F. Qiu, S. Fujita, R. Mhanna, L. Zhang, B. R. Simona, B. J. Nelson, *Adv. Funct. Mater.* **2015**, *25*, 1666.
[5] S. Fusco, H.-W. Huang, K. E. Peyer, C. Peters, M. Häberli, A. Ulbers, A. Spyrogianni, E. Pellicer, J. Sort, S. E. Pratsinis, B. J. Nelson, M. S. Sakar, S. Pane, *ACS Appl. Mater. Interfaces* **2015**, *7*, 6803.
[6] S. Fusco, M. S. Sakar, S. Kennedy, C. Peters, R. Bottani, F. Starsich, A. Mao, G. A. Sotiriou, S. Pané, S. E. Pratsinis, D. Mooney, B. J. Nelson, *Adv. Mater.* **2014**, *26*, 952.
[7] E. Gultepe, J. S. Randhawa, S. Kadam, S. Yamanaka, F. M. Selaru, E. J. Shin, A. N. Kalloo, D. H. Gracias, *Adv. Mater.* **2013**, *25*, 514.
[8] S. Pedron, S. van Lierop, P. Horstman, R. Penterman, D. J. Broer, E. Peeters, *Adv. Funct. Mater.* **2011**, *21*, 1624.
[9] G. Z. Lum, Z. Ye, X. Dong, H. Marvi, O. Erin, W. Hu, M. Sitti, *Proc. Natl. Acad. Sci. U. S. A.* **2016**, *113*, E6007.
[10] W. Hu, G. Z. Lum, M. Mastrangeli, M. Sitti, *Nature* **2018**, *554*, 81.
[11] K. E. Peyer, E. C. Siringil, L. Zhang, M. Suter, B. J. Nelson, *Lect. Notes Comput. Sci.* **2013**, *8064*, 216.
[12] C. Peters, O. Ergeneman, P. D. W. García, M. Müller, S. Pané, B. J. Nelson, C. Hierold, *Adv. Funct. Mater.* **2014**, *24*, 5269.
[13] J. Kim, S. E. Chung, S. E. Choi, H. Lee, J. Kim, S. Kwon, *Nat. Mater.* **2011**, *10*, 747.
[14] S. R. Mishra, M. D. Dickey, O. D. Velev, J. B. Tracy, *Nanoscale* **2016**, *8*, 1309.
[15] H.-W. Huang, M. S. Sakar, K. Riederer, N. Shamsudhin, A. Petruska, S. Pane, B. J. Nelson, *IEEE International Conference on Robotics and Automation*; IEEE, Stockholm, Sweden **2016**.
[16] F. Popp, J. P. Armitage, D. Schüler, *Nat. Commun.* **2014**, *5*, 5398.
[17] M. Chariaou, L. Rahn-Lee, J. Kind, I. García-Rubio, A. Komeili, A. U. Gehring, *Biophys. J.* **2015**, *108*, 1268.
[18] L. Yan, S. Zhang, P. Chen, H. Liu, H. Yin, H. Li, *Microbiol. Res.* **2012**, *167*, 507.
[19] R. M. Erb, R. Libanori, N. Rothfuchs, A. R. Studart, *Science* **2012**, *335*, 199.
[20] R. M. Erb, J. S. Sander, R. Grisch, A. R. Studart, *Nat. Commun.* **2013**, *4*, 1712.
[21] M. A. Ward, T. K. Georgiou, *Polymers (Basel)* **2011**, *3*, 1215.
[22] H.-W. Huang, M. S. Sakar, A. J. Petruska, S. Pane, B. J. Nelson, *Nat. Commun.* **2016**, *7*, 1.
[23] M. Charilaou, *J. Appl. Phys.* **2017**, *122*, 63903.
[24] M. P. Jummer, J. J. Abbott, B. E. Kratochvil, R. Borer, A. Sengul, B. J. Nelson, *IEEE International Conference on Robotics and Automation*; IEEE, Alaska, USA **2010**, p. 1610.